AAS 16-464

LUNAR ADVANCED RADAR ORBITER FOR SUBSURFACE SOUNDING (LAROSS): LAVA TUBE EXPLORATION MISSION

Rohan Sood[*], H. Jay Melosh[†], and Kathleen Howell[‡]

With the goal of expanding human presence beyond Earth, sub-surface empty lava tubes on other worlds form ideal candidates for creating a permanent habitation environment safe from cosmic radiation, micrometeorite impacts and temperature extremes. In a step towards Mars exploration, the Moon offers the most favorable pathway for lava tube exploration. In-depth analysis of GRAIL gravity data has revealed several candidate empty lava tubes within the lunar maria. The goal of this investigation is a proposed subsurface radar sounding mission to explore the regions of interest and potentially confirm the presence and size of buried empty lava tubes under the lunar surface.

INTRODUCTION

NASA's successful Gravity Recovery and Interior Laboratory (GRAIL) has determined the lunar gravity field to an unprecedented precision.[1] Through gravitational analysis of the Moon, subsurface features, including potential buried empty lava tubes, have been detected.[2] Lava tubes create an interest as possible human habitation sites safe from cosmic radiation, micrometeorite impacts and temperature extremes. The existence of such natural caverns is supported by Kaguya's discoveries of deep pits that may potentially be openings to empty lava tubes.[3] The goal of this investigation is a proposed sub-surface radar sounding mission to potentially confirm the presence and size of buried empty lava tubes under the lunar surface. The high resolution gravity field derived from the GRAIL data will allow a spacecraft to accurately navigate at altitudes of 10 to 20 km over the mare regions. The radar sounder system is designed to penetrate the lunar surface from a few meters to a few kilometers in search of signatures that can confirm the presence, depth and extent of an empty lava tube. The results will be compared to the findings from GRAIL gravity analysis and the locations of known lunar skylights. Once detection is confirmed, such sites can be assessed for future human habitation and exploration on the Moon, Mars, and beyond.

[*]Ph.D. Candidate, School of Aeronautics and Astronautics, Purdue University, 701 West Stadium Avenue, West Lafayette, IN 47907-2045, USA. rsood@purdue.edu

[†]Distinguished Professor EAS/Physics, Department of Earth, Atmospheric and Planetary Sciences, Purdue University, 550 Stadium Mall Drive, West Lafayette, Indiana 47907-2051, USA. 765-494-3290, jmelosh@purdue.edu

[‡]Hsu Lo Distinguished Professor of Aeronautics and Astronautics, School of Aeronautics and Astronautics, Purdue University, 701 West Stadium Avenue, West Lafayette, IN 47907-2045, USA. 765-494-5786, howell@purdue.edu

SCIENTIFIC INTEREST

With the goal of expanding human presence beyond Earth, buried empty lava tubes on other worlds form ideal candidates for creating a permanent habitation environment. The lunar surface, unprotected by an atmosphere, is vulnerable to both direct and secondary meteoroid impacts and is exposed to cosmic and solar particle radiation that pose severe challenges to a lunar base on the surface.[4] With multiple layers of lava basalt forming a meters-thick roof, buried empty lava tubes can supply a safe zone away from life-threatening conditions. The ambient temperature in a lava tube is nearly constant, in contrast to the extremes on the lunar surface.[5] In addition to the protection afforded by buried lunar lava tubes, siting habitats in such caverns can lower the cost associated with setting up a habitat on the lunar surface sufficiently safe for humans with the aim of providing a stable environment for long-term/permanent lunar habitation.[4] Lunar lava tubes also offer a pristine environment to examine a part of the Moon untouched by the extremities and impurities introduced by micrometeorites to which the lunar surface is continuously exposed. Such an environment can also add insight concerning the lunar history and facilitate careful examination of its composition.

Potential buried lava tubes and skylights have also been detected on Mars.[6,7] Possible lava tube structures were first recognized in the images from the Viking orbiter. Subsequent observation and identification were obtained by Mars Odyssey, Mars Global Surveyor, Mars Express and Mars Reconnaissance Orbiter.[8–10] Prior to a journey to Mars with the goal of colonizing the planet, it is vital to analyze the potential of exploiting lava tubes as habitation sites. Although Mars does possess an atmosphere, it is extremely thin, the surface is exposed to cosmic radiation, undergoes huge temperature swings, and experiences occasional storms that often extend across most of the planet.[11,12] Such conditions can be devastating and prove fatal on the Martian surface. To prevent exposure to such life-threatening events, and to reduce the cost of setting up human habitats on the surface of the Mars, it is beneficial to explore Martian lava tubes as potential sites for future human habitats. Thus, in a step towards Mars exploration, the Moon offers the most favorable pathway for lava tube exploration as future human habitats beyond the Earth.

In addition to the benefit of safe habitation sites on both the Moon and the Mars, buried lava tubes, with potential access through a skylight, can also allow harvesting underground mineral resources.[13] Subsurface caverns can be explored and natural resources exploited without excavation. Given that these sites grant ambient temperatures, in contrast to those on the surface, some researchers suggest that, if life does exist on Mars, it is likely to be detected in the habitable environment of subsurface empty lava tubes.[14,15] Essential life-supporting volatiles, such as water, could potentially be trapped in these subsurface caverns creating a more hospitable life-supporting environment. Thus, exploration of lava tubes on Mars is a significant goal for the scientific community as an opportunity to explore the Martian subsurface history and astrobiological past.

MISSION GOALS

In-depth analysis of GRAIL gravity data has revealed several candidate empty lava tubes within the lunar maria. The goal of the proposed mission is a subsurface radar sounder in orbit around the Moon to further explore the regions of interest and potentially validate the existence of candidate lava tubes. Additional lava tube candidates may be detected, particularly those beyond the resolution of the GRAIL gravity data. The radar sounder system will map the entire mare from a few meters to few kilometers below the lunar surface. Positive confirmation of buried empty lava tubes on the Moon, with possible access as habitation sites, would offer scientists, engineers, and astronauts an opportunity to examine the environment and satisfy crucial exploration goals identified in the roadmap to Mars.[16] The data from the envisioned subsurface sounder might also support science inquiries, such as the nature of the enigmatic mare ridges, the location of the feeder dikes for lava eruptions, as well as the depth and extent of impact melt in large lunar craters.

Examining the structure of lunar volcanic vents, where the Moon's internal heat resulted in massive volcanic eruptions, is also gaining interest.[17] A large number of features resembling vents similar to shield volcanoes have been detected within the 2,500 km wide Oceanus Procellarum, particularly on and around the Aristarchus plateau.[18] GRAIL data analysis suggests that Procellarum may be flooded by large volcanic eruptions caused by Moon's internal heat. The proposed feeder dikes for these lavas lie in a large system that follows the outline of Oceanus Procellarum.[19] Within Oceanus Procellarum lies the very distinct Aristarchus plateau comprised of both low and high reflectance terrain units.[20] The plateau is surrounded by lava flows and the region itself is covered by a large number of sinuous rilles, characterized by meandering channels of varying widths and depths. The rilles are often associated with the presence of depressions of various morphology that are interpreted as potential source vents for the lava flow that initially formed the lavas that flowed through the channels.[21] One of the largest lunar rilles, Vallis Schröteri lies within the Aristarchus plateau. This rille originates from a feature that resembles a 'cobra head' that consists of a deep pit and is thought to be the source of a massive lava outflow that meandered across the Aristarchus plateau and formed Vallis Schröteri.[22] The rille ends abruptly with no surface expression. GRAIL data analysis has demonstrated a potentially uncollapsed buried lava tube that extends beyond the visible surface expression.[2] The radar mission can assist in understanding and deciphering the mystery beneath structures of volcanic vents as well as explore specific target areas along with a general survey in search for buried empty lava tubes.

PREVIOUS GROUND PENETRATING RADAR MISSIONS

Ground penetrating radar serves to meet a variety of multidisciplinary scientific goals. With transmitted radio waves, ground penetrating radar can probe deep into the subsurface and reflect electromagnetic waves off layers and structures of varying dielectric constant. The returned waves are received and processed to map the subsurface of the body of interest.

Apollo Lunar Sounder Experiment (ALSE):

In 1972, a ground penetrating radar via the Apollo Lunar Sounder Experiment, was flown on NASA's Apollo 17 mission. Radar waves at three different frequencies were transmitted to examine the lunar surface and interior. As with any radar-based mission, the choice of frequencies (5, 15, and 150 MHz) was critical in decision-making to produce a balance between the desired resolution and the penetration depth. Longer wavelengths (lower frequencies) penetrate deeper below the surface, whereas shorter wavelengths (higher frequencies) yield higher resolution to differentiate between the echoes.

The main objective of the ALSE was exploration of the upper 2 km of the lunar crust. The lack of water on the Moon enabled deeper penetration using the longer wavelengths than is possible on Earth. Shorter wavelengths assist in generating surface images and lunar profiles. The data analysis led to precise topographic information and revealed several structures under the lunar maria. The experiment yielded some initial estimates for the thickness of the basaltic layers and lava flows.[23] An improved, but not sufficient, understanding of the mare ridges (also known as wrinkle ridges) allowed geologists to speculate on the formation of these long, low lunar ridges supporting the hypothesis that their formation was a result of motion along faults cutting through the mare lavas.

Mars Advanced Radar for Subsurface and Ionosphere Sounding (MARSIS):

On-board ESA's Mars Express spacecraft, MARSIS is a low frequency radar sounder designed to assess the Martian subsurface with the aim of locating frozen water. Deployed in 2005, MARSIS enabled differentiation between the dielectric constant of the northern and southern high-latitude regions.[24] This radar operated in the 1–5 MHz frequency range. The low frequency permitted the waves to penetrate deeper, up to depths of 5 km, allowing exploration of Martian crustal properties, geological processes, subsurface ice and liquid water. The data also suggested that the northern basin is filled with low density material that can possibly be interpreted as evidence for an ancient northern ocean. Although the radar has the advantage of penetrating deep below the Martian surface, MARSIS has a relatively coarse resolution. The need to further explore the top few hundreds of meters below the Martian surface prompted a need for an instrument to complement the results of MARSIS by providing finer resolution of the top 10-20 meters to understand the sedimentary processes and geologic activity.

Mars SHAllow RADar sounder (SHARAD):

The Italian Space Agengy's SHAllow RADar on NASA's Mars Reconnaissance Orbiter (MRO) is a subsurface sounding radar that was launched in 2005. The experiment is designed to investigate the Martian subsurface near the polar ice caps and carry out a global survey in a search for underground ice and liquid water by examining the subsurface interfaces. SHARAD operates at a central frequency of 20 MHz with a 10 MHz bandwidth that complements the findings from MARSIS and characterizes the upper km of the Martian surface with greater resolution. The experiment also aims to estimate surface roughness at scales 10–100 m to assess the physical properties, landing safety and site trafficability.[25]

Lunar Radar Sounder (LRS):

For subsurface observations of the lunar interior, the Lunar Radar Sounder experiment flew onboard the Japanese Kaguya (SELENE) spacecraft in 2009. The instrument operated throughout most of the nominal mission during which low frequency (5 MHz) waves were used to map and characterize the lunar subsurface under the maria.[26] The LRS was equipped with two sets of 30 m dipole antennas. The low frequency waves enabled mapping the subsurface to a depth of several km but the resolution was on the order of 100 m. The primary objective of the LRS mission was to investigate the thermal history of the Moon and understand its evolution over a time scale of hundreds of millions of years. As a result, the observations revealed stratification and tectonic features under the lunar surface that may assist in understanding the thermal evolution of the Moon.

Ground Penetrating Radar (GPR):

In 2013, China's Yutu rover on-board the Chang'e 3 spacecraft was the first to carry out direct measurements of the Moon's near-surface structures with a ground penetrating radar attached to the underbelly of the Yutu rover. The radar operated at central frequencies of 60 and 500 MHz permitting a range resolution of 3.75 and 0.3 m, respectively.[27,28] The data from the radar instrument suggested a 1 m thick reworked zone underlain by a 2-6 m thick ejecta layer near the landing site within northern Mare Imbrium. The rover covered a total distance of 114 meters over two lunar days. Due to mechanical issues associated with the rover controls, no further area was traversed.

INSTRUMENT AND FRAMEWORK

Radar sounding from lunar orbit offers global coverage of the vast mare region. High precision and accurate knowledge of the GRAIL gravity data permits the spacecraft to fly at much lower altitudes than previous orbital missions over the regions of interest. Multiple, low altitude revolutions over the same area can supply the large data sets that are essential for unambiguous 3-D mapping of the lunar subsurface. To compliment the polar orbit selected for the GRAIL spacecraft, the radar sounder is proposed to fly in an inclined orbit as plotted in Figure 1. Due to the GRAIL spacecraft's polar orbit, high resolution data highlighted individual tracks appearing as a North-South striping that interfered with the ability to recognize weak North-South trending linear or sinuous features. Selection of an inclined trajectory for the radar-based spacecraft may prevent such North-South artifacts and can potentially reveal additional subsurface features that were not recognized with the GRAIL data analysis. In addition, placing the spacecraft in an eccentric orbit, the aim of flying relatively low over the lunar maria to maximize the resolution, while flying high over the farside highlands can be realized. In Figure 1, the spacecraft is flying at an altitude of approximately 20-25 km over the mare region with an estimated orbital inclination of 60°.

As a part of designing and analyzing the Ground Penetrating Radar (GPR), the components and functions of a GPR must be understood. The instrument is based on a geophysical technique that involves transmitting a radio signal into the ground and monitoring the wave returned by reflection at the surface and subsurface boundaries. A standard GPR consists of

Figure 1: Low altitude orbits over mare region for global coverage.

a transmitting antenna linked to a source from which radio waves are emitted in the direction of the region under study. The amplitude of the waves reflected from various depths and boundaries with different dielectric constants, is gauged by the receiving antenna in conjunction with a signal processing system. The processed data are then telemetered to Earth for further processing and a 3-D reconstruction of the subsurface using data from adjacent orbital tracks.

The primary goal of the mission is a map of the lunar subsurface in search of signals that are consistent with buried empty lava tubes. The most critical trade-off in designing the instrument is, therefore, resolution versus penetration depth. High resolution data requires higher frequency (shorter wavelength) waves to be emitted. However, short wavelengths penetrate less deeply into the lunar surface. Because this investigation aims to penetrate the lunar surface to a depth of a few kilometers, long wavelength signals will be emitted, requiring long antennas on the spacecraft. In contrast to conditions on the Earth, where ground water is abundant, the lunar crust is very dry, making it easier for the radar waves to penetrate much deeper under the surface. With the knowledge of surface topography, late returns appearing in the data may be interpreted as subsurface returns. Multiple tracks, in conjunction with modern 3-D processing techniques, will enable reliable reconstruction of the subsurface structure. Radio waves are reflected and returned as echoes by subsurface boundaries, defined by contrasting dielectric properties of the traversed medium, as illustrated in Figure 2. The transmitter sends a signal towards the surface from the spacecraft orbit at altitude, h. The first reflection is from the surface and the subsequent echoes are generated by subsurface boundaries between different mediums at various depths. The receiver picks up the returning echoes from both surface and subsurface boundaries. By

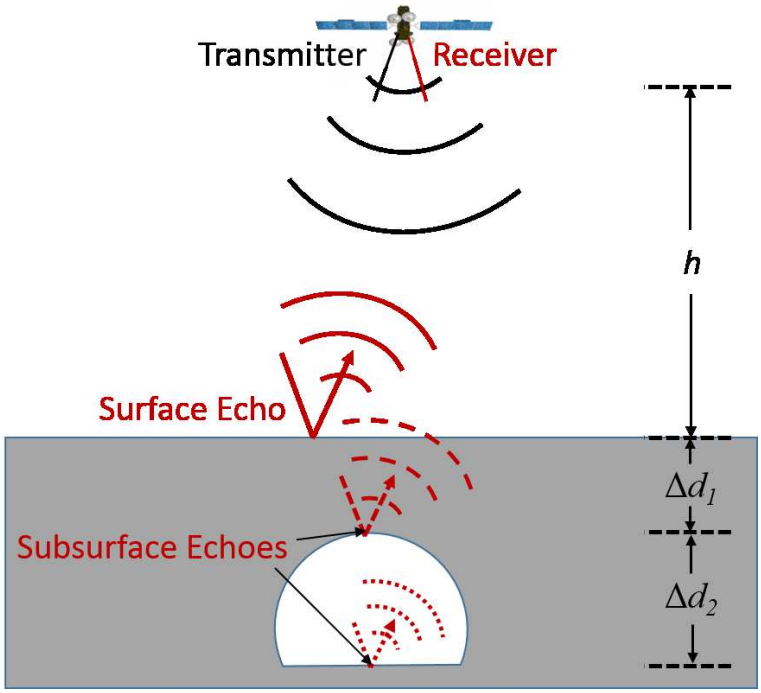

Figure 2: Schematic for GPR transmitting and receiving wave signal from lunar orbit.

analyzing the echoes generated, delay times can be converted to the depths of subsequent boundaries on a sample-by-sample basis using

$$\Delta d_i = \frac{1}{2}\Delta t c \epsilon_i^{-1/2} \tag{1}$$

where Δd_i is the depth interval for the $i-$th sample, Δt is the delay-time sampling interval, c is the speed of light, and ϵ_i is the dielectric constant of the traversed medium.[25] The factor of $1/2$ accommodates the two-way distance traveled by the wave.

The shortest possible pulse is not always ideal for achieving the desired range resolution. Orbiting radars exploit a signal shaping strategy, called chirp, that employs a long pulsating signal linearly modulated in frequency. The vertical resolution of the radar, ρ_z, is defined as

$$\rho_z = \frac{c}{2B_w\sqrt{\epsilon_i}} \tag{2}$$

where B_w is the bandwidth of the transmitted pulse.[29] A similar signal shaping technique was adopted by SHAlow RADar (SHARAD) subsurface sounding radar aboard the Mars Reconnaissance Orbiter (MRO). The transmitter emits a 10 W, 85 μs chirped pulse centered at 20 MHz with 10 MHz bandwidth. The configuration yields vertical and horizontal resolutions of $\sim$7 m and 0.3–1 km $\sim$ 3–7 km (along-track $\sim$ cross-track), respectively. Though the frequency band resulted in higher resolution, the penetration depth was limited

to ∼1 km. To compliment SHARAD, the Mars Advanced Radar for Subsurface and Ionosphere Sounding (MARSIS) spacecraft operated at a frequency range of 1–5 MHz, capable of penetrating up to 5 km under the surface of the MARS, but the instrument was limited by range resolution.[30] In 1972, the GPR experiment that flew aboard Apollo 17 was capable of penetrating the lunar surface up to a depth of 1.3 km with 100 m range resolution operating at frequencies of 5, 15 and 150 MHz.[31] The penetration depths of the radar sounder aboard JAXA's 2007 SELenological and ENngineering Explorer (SELENE) was 5 km with 75 m range resolution operating at 4–6 MHz.[32] Thus, an appropriate balance between the data resolution and penetration depth is desirable.

These previous missions demonstrate the feasibility of deep penetration of the lunar surface with relatively low power transmitters. These missions have already produced data about the dielectric constant for the lunar surface lavas (for both real and imaginary parts) at a number of relevant frequencies. The proposed mission will exceed the performance of these radars, however, mainly because of the low altitudes as a consequence of the high-precision GRAIL gravity field that enables safe navigation at altitudes of 10 km or less, a capability already demonstrated as part of the GRAIL Extended mission.[33–35] Like all radars, the returned signal strength is proportional to the inverse fourth power of the distance between the transmitter and receiver, so that decreasing altitude from the minimum altitude of 50 km for Kaguya (or about 100 km for the Apollo 17 command module orbit) down to 10 km yields an increase in signal strength by a factor of 625, which will greatly enhance detection of discontinuities below the lunar surface.

PRELIMINARY RESULTS FROM GRAIL GRAVITY SURVEYS

General Survey

With high resolution topography and gravitational data available for the Moon, it is now possible to recognize the gravitational footprints that may correspond to subsurface density anomalies. Topography data from Lunar Orbiter Laser Altimeter (LOLA), for a vast region of interest covering Oceanus Procellarum, appears in Figure 3a. Topography and surface imagery do not allow detection of subsurface features such as empty lava tubes. Thus, the GRAIL gravity data is exploited to detect the mass deficit associated with buried empty lava tubes. A numerical strategy based on the gradiometry technique has been developed to assist in the detection of subsurface features.[2] The technique exploits gravity gradients and the computation of eigenvalues and eigenvectors associated with the Hessian matrix which consists of the second horizontal derivatives of the gravity potential. The Bouguer gravity potential (equal to the observed potential minus that associated with topography) is analyzed by developing eigenvalue maps that depict the magnitude and direction of gravity at each point on the grid as apparent in Figure 3b. As a consequence of the second derivative in the computation of the Hessian, a negative anomaly (mass deficit) corresponds to a positive eigenvalue on the map. Thus, the color scale in Figure 3b represents the signed magnitude of the largest magnitude eigenvalue of the Hessian derived from the gravitational potential. The maps are produced by averaging three different gravity models representing the same initial harmonic data with different lower and upper wavelength truncations to

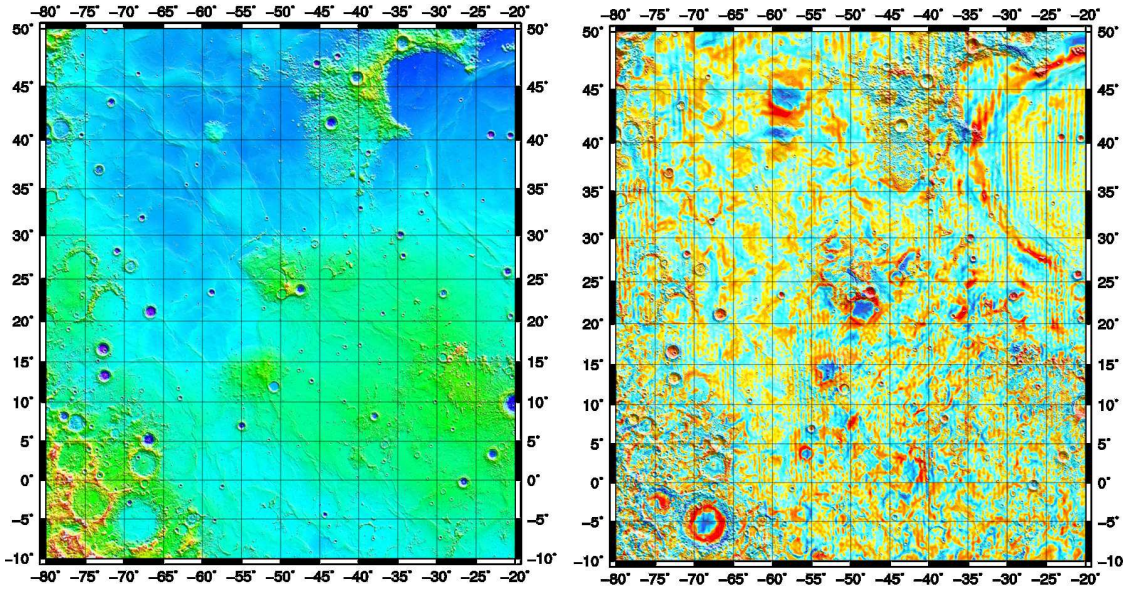

(a) Oceanus Procellarum topography. (b) Maximum eigenvalue map for Bouguer potential.

Figure 3: Topographic and gradiometry (applied to Bouguer potential) comparison for the Oceanus Procellarum region.

attenuate the resulting ringing. Only the higher harmonic coefficients are evaluated to eliminate gradual regional variations in the gravity potential: The small structures are sought such that the associated gravity anomalies will posses short spatial wavelengths. Various structures emerge due to the gravity variations, ones that are not evident from surface topography. A secondary detection strategy, cross-correlation, utilizes the individual track data based on the relative acceleration between the two spacecraft as they move along their respective orbits. The observed accelerations are then cross-correlated with the signal expected from a long, empty cylinder below the Moon's surface. Because of the near-polar orbit of the GRAIL spacecraft, this technique is most sensitive to lava tubes oriented in an East-West direction. The gradiometry and cross-correlation detection techniques are applied to localized regions. Gravity models up to degree and order 1080, with predetermined truncation and tapers, are utilized.

Target Areas

Detected Candidates: GRAIL gravity data analysis has led to the detection of underground empty structures whose signature resembles that of empty lava tubes. Within this context, several regions in the maria with known sinuous rilles are considered, in particular, a region around the known Marius Hills skylight (301-307°E, 11-16°N). Cross-correlation analysis of this region appears in Figure 4, with the red dot marking the location of a known skylight along the rille. The bottom-left map in Figure 4 corresponds to the correlation between free-air and Bouguer maps where a strong correlation (red) is indicative of potential underground features. However, the structures that are the object of this analysis are on a

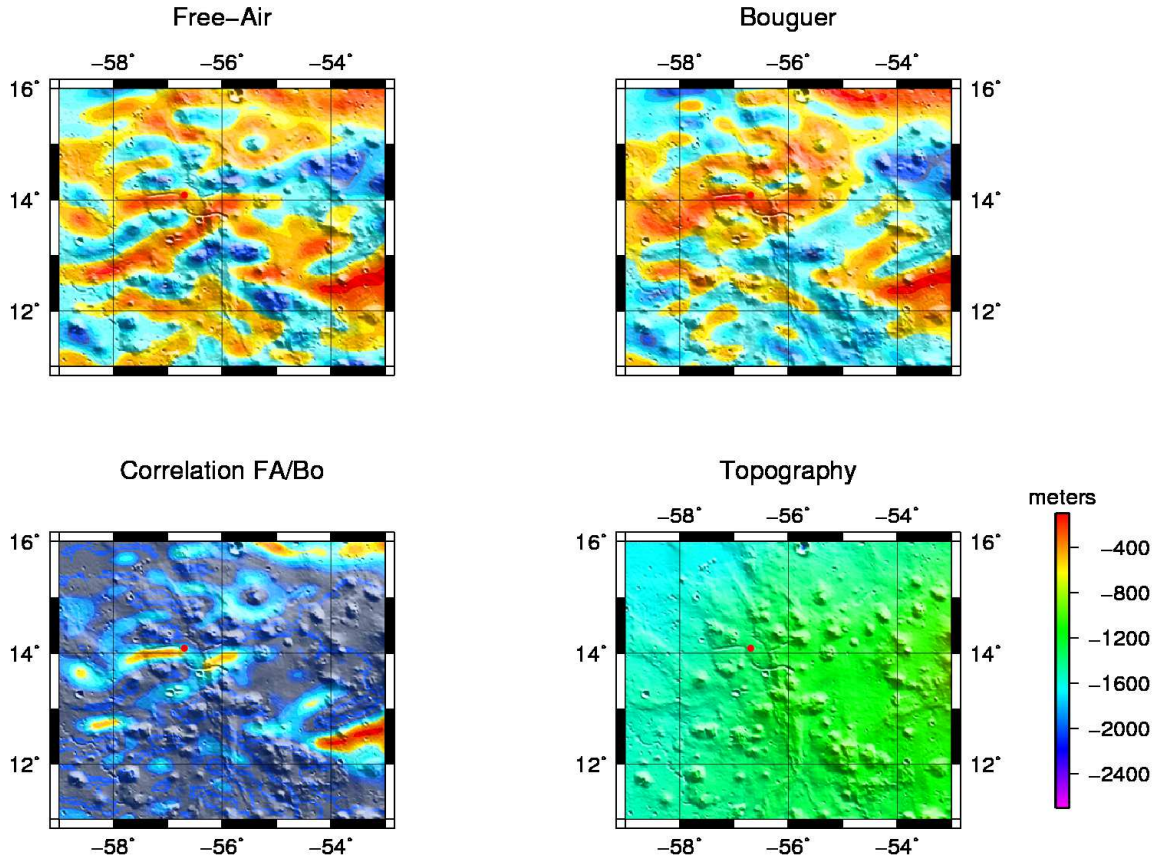

Figure 4: Free-air and Bouguer cross-correlation maps and free-air/Bouguer correlation along with regional topography in the vicinity of Marius Hills skylight.

scale similar or smaller than the resolution of the gravity data. It is, therefore, challenging to determine whether a signal observed on an eigenvalue or cross-correlation map is, in fact, the signature of a physical structure or is a numerical artifact. To assess the robustness of an observed signal, rather than considering a single simulation, several different spherical harmonic solutions, truncated between various lower and upper degrees, are considered to produce a collection of maps. The cross-correlation maps in the top row and the bottom-left of Figure 4 yield an averaged map over a few hundred simulations. The bottom-right map supplies a visual reference for the regional topography along with elevation in the vicinity of Marius Hills skylight.

The capability of both strategies to identify subsurface anomalies has led to the detection of additional candidate structures within the lunar maria. A region around a newly found lunar pit in Sinus Iridum appears in Figure 5. The top row of Figure 5 illustrates the corresponding local averaged maximum eigenvalues for the free-air, Bouguer potentials, and the correlation between the two. The red dot marks the location of a newly identified pit/skylight (331.2°E, 45.6°N) within Sinus Iridum. The pit itself is approximately 20 m deep with central hole of 70 m x 33 m and an outer funnel of 110 x 125 m. The maps overlie local topography, and the color represents the signed magnitude corresponding to

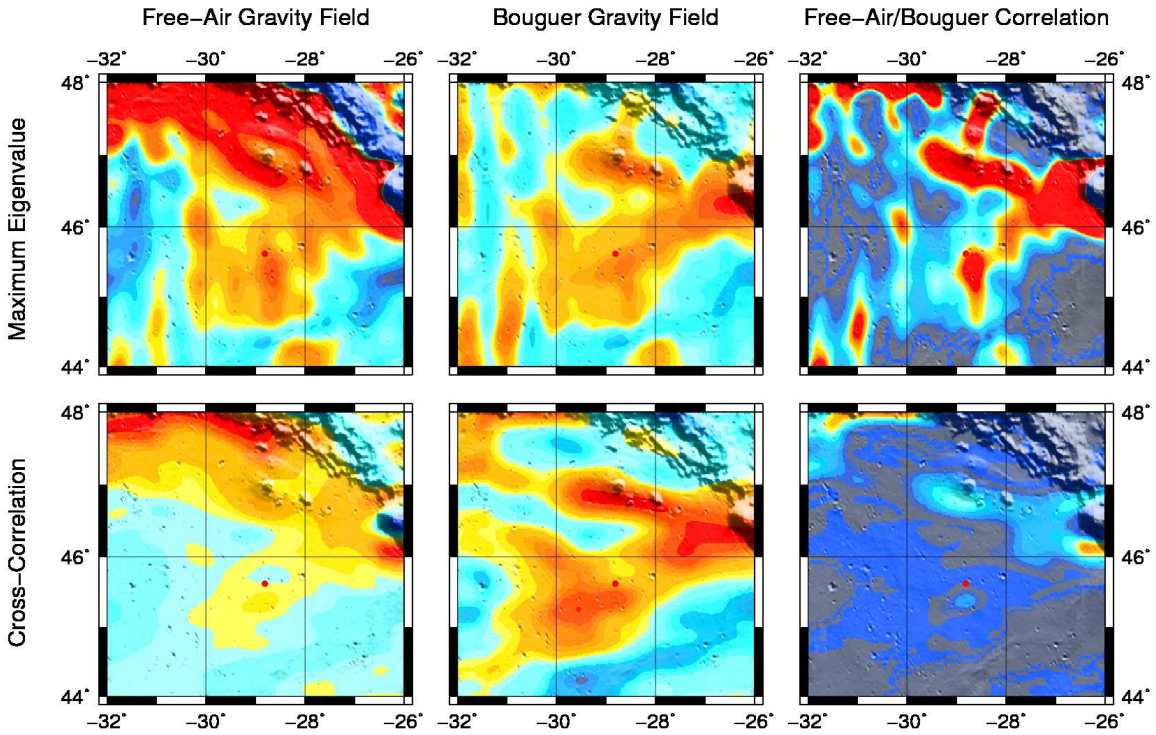

Figure 5: Local gradiometry (top), cross-correlation (bottom) maps for free-air (left), Bouguer (center), and free-air/Bouguer correlation (right) for Sinus Iridum pit.

the largest eigenvalue of the Hessian derived from the gravitational potential. Both free-air and Bouguer eigenvalue maps highlight a gravity low in the vicinity of the lunar pit. The correlation map distinctively marks the region near the pit as a region of mass deficit with a potential access to an underground cavity. The cross-correlation technique results appear in the second row of Figure 5. The schematic demonstrates that for both free-air and Bouguer cross-correlation maps, the anomaly is detected in the same region as deduced from the gradiometry technique. Both strategies offer evidence for a subsurface mass-deficit anomaly in the vicinity of the newly found lunar pit.

Free-air and Bouguer Gravity Anomaly: Continuing the validation of the subsurface ano-maly, regional free-air and Bouguer gravity maps are generated. Figure 6 illustrates local maps for the free-air gravity on the left and Bouguer gravity on the right. Upon closer inspection, the two gravity maps demonstrate a gravity low surrounding the rille that includes the Marius Hills skylight. The Bouguer low adds to the evidence suggesting a potential buried empty lava tube along the rille with an access through the Marius Hills skylight. Similar free-air and Bouguer gravity analysis is completed for the newly identified pit in Sinus Iridum as illustrated in Figure 7. The color bar is adjusted to visually distinguish the region in proximity to the lunar pit in Sinus Iridum. The gravity low in both the free-air and Bouguer gravity suggests an underground mass deficit in the vicinity of the pit. Although the pit itself is relatively small, it can potentially afford access to a larger underground structure as evident from the gravity maps and both detection strategies. Ad-

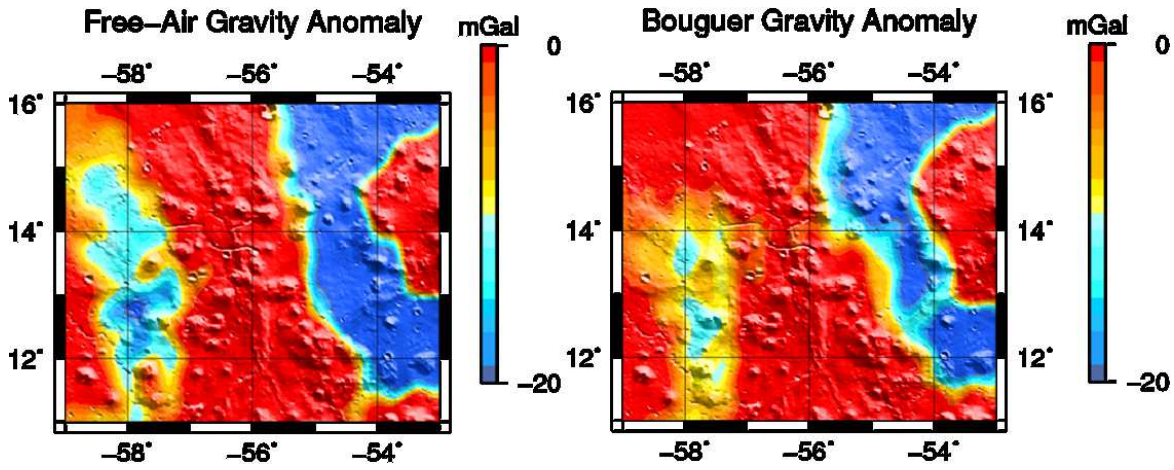

Figure 6: Local free-air (left) and Bouguer (right) gravity map for Marius Hills skylight with overlay of topography.

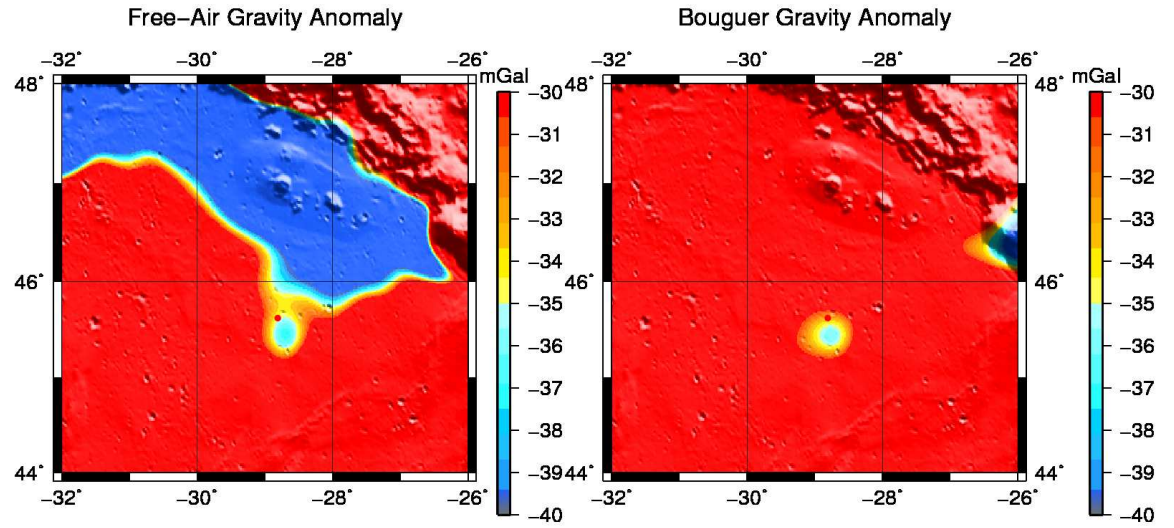

Figure 7: Local free-air (left) and Bouguer (right) gravity map for the newly found lunar pit in Sinus Iridum with overlay of topography.

ditional maps have also been examined to identify a possible connection of this anomaly to a buried empty lava tube structure.

The techniques have been extended to cover the vast mare regions of Oceanus Procellarum. Multiple new candidates for buried empty lava tube structures have emerged as part of a broader investigation. Some of the lava tube candidates possess no surface expression but similar signals are, in fact, observed from both detection strategies, as observed for candidates with clear surface expressions, i.e., skylights/pits.

CONCLUSIONS

As a result of the subsurface gravity gradient analysis, several candidate sites have been recognized with a gravitational signature similar to that of a buried empty lava tube. Some of these sites are in the vicinity of known sinuous rilles and skylights visible on the lunar surface. Although the GRAIL mission did result in determining the lunar gravity to an unprecedented precision, small scale features, such as smaller lava tubes and skylights, are beyond the resolution of the data. In addition, the near polar orbit of the GRAIL spacecraft introduced a North-South bias in the measurements. The Lunar Advanced Radar Orbiter for Subsurface Sounding (LAROSS) spacecraft offers an extension of the findings of the GRAIL mission by exploring sites with potentially buried empty lava tubes and an expansion of the process to the whole mare region in search of smaller lava tubes. The low altitude passes of the radar sounder over the mare region will aid in obtaining better resolution and penetrating deeper below the lunar surface. This experiment will assist in the search for buried empty lava tubes that may offer the potential to access and construct habitats, safe from harsh surface environment and, thus, enabling future human exploration.

ACKNOWLEDGMENTS

The research work described in this paper made use of GRAIL data and was carried out at Purdue University. The GRAIL mission is supported by the NASA Discovery Program under contract to the Massachusetts Institute of Technology and the Jet Propulsion Laboratory, California Institute of Technology.

REFERENCES

[1] M. T. Zuber, D. E. Smith, D. H. Lehman, T. L. Hoffman, S. W. Asmar, and M. M. Watkins, "Gravity Recovery and Interior Laboratory (GRAIL): Mapping the lunar interior from crust to core," *Space Science Reviews*, Vol. 178, No. 1, 2013, pp. 3–24.

[2] L. Chappaz, R. Sood, K. C. Howell, and H. J. Melosh, "Buried Empty Lava Tube Detection with GRAIL Data," *AIAA/AAS Astrodynamics Specialist Conference Conference and Exposition*, American Institute of Aeronautics and Astronautics (AIAA), aug 2014.

[3] J. Haruyama, K. Hioki, M. Shirao, T. Morota, H. Hiesinger, C. H. v. d. Bogert, H. Miyamoto, A. Iwasaki, Y. Yokota, M. Ohtake, *et al.*, "Possible lunar lava tube skylight observed by SELENE cameras," *Geophysical Research Letters*, Vol. 36, No. 21, 2009.

[4] D. G. Angelis, J. Wilson, M. Clowdsley, J. Nealy, D. Humes, and J. Clem, "Lunar lava tube radiation safety analysis," *Journal of radiation research*, Vol. 43, No. Suppl, 2002, pp. S41–S45.

[5] C. L. York, B. Walden, T. L. Billings, and P. D. Reeder, "Lunar lava tube sensing," *New Technologies for Lunar Resource Assessment*, Vol. 1, 1992, pp. 51–52.

[6] G. Cushing, T. Titus, J. Wynne, and P. Christensen, "THEMIS observes possible cave skylights on Mars," *Geophysical Research Letters*, Vol. 34, No. 17, 2007.

[7] R. J. Léveillé and S. Datta, "Lava tubes and basaltic caves as astrobiological targets on Earth and Mars: a review," *Planetary and Space Science*, Vol. 58, No. 4, 2010, pp. 592–598.

[8] L. Keszthelyi, W. Jaeger, A. McEwen, L. Tornabene, R. A. Beyer, C. Dundas, and M. Milazzo, "High Resolution Imaging Science Experiment (HiRISE) images of volcanic terrains from the first 6 months of the Mars Reconnaissance Orbiter primary science phase," *Journal of Geophysical Research: Planets (1991–2012)*, Vol. 113, No. E4, 2008.

[9] C. Parcheta, "Lava flows in the Tharsis region of Mars: estimates of flow speeds and volume fluxes," *HSGC Report Number 06-14*, 2005, p. 88.

[10] J. Bleacher, R. Greeley, D. Williams, and G. Neukum, "Comparison of effusive volcanism at Olympus, Arsia, Pavonis, and Ascraeus Montes, Mars from lava flow mapping using Mars Express HRSC data," *37th Lunar and Planetary Science Conference. Abstract*, Vol. 1182, 2006.

[11] L. C. Simonsen, J. E. Nealy, L. W. Townsend, and J. W. Wilson, "Radiation exposure for manned Mars surface missions," tech. rep., National Aeronautics and Space Administration, Hampton, VA (USA). Langley Research Center, 1990.

[12] B. A. Cantor, P. B. James, M. Caplinger, and M. J. Wolff, "Martian dust storms: 1999 Mars orbiter camera observations," *Journal of Geophysical Research: Planets (1991–2012)*, Vol. 106, No. E10, 2001, pp. 23653–23687.

[13] B. E. Walden, T. L. Billings, C. L. York, S. L. Gillett, and M. V. Herbert, "Utility of lava tubes on other worlds," *Using in situ Resources for Construction of Planetary Outposts*, Vol. 1, 1998, p. 16.

[14] A. G. Fairén, J. M. Dohm, E. R. Uceda, A. P. Rodríguez, V. R. Baker, D. Fernández-Remolar, D. Schulze-Makuch, and R. Amils, "Prime candidate sites for astrobiological exploration through the hydrogeological history of Mars," *Planetary and Space Science*, Vol. 53, No. 13, 2005, pp. 1355–1375.

[15] D. Schulze-Makuch, L. N. Irwin, J. H. Lipps, D. LeMone, J. M. Dohm, and A. G. Fairén, "Scenarios for the evolution of life on Mars," *Journal of Geophysical Research: Planets (1991–2012)*, Vol. 110, No. E12, 2005.

[16] J. Blamont, "A roadmap to cave dwelling on the Moon and Mars," *Advances in Space Research*, Vol. 54, No. 10, 2014, pp. 2140–2149.

[17] J. W. Head and A. Gifford, "Lunar mare domes: classification and modes of origin," *The moon and the planets*, Vol. 22, No. 2, 1980, pp. 235–258.

[18] P. D. Spudis, P. J. McGovern, and W. S. Kiefer, "Large shield volcanoes on the Moon," *Journal of Geophysical Research: Planets*, Vol. 118, No. 5, 2013, pp. 1063–1081.

[19] J. C. Andrews-Hanna, J. Besserer, J. W. Head III, C. J. Howett, W. S. Kiefer, P. J. Lucey, P. J. McGovern, H. J. Melosh, G. A. Neumann, R. J. Phillips, *et al.*, "Structure and evolution of the lunar Procellarum region as revealed by GRAIL gravity data," *Nature*, Vol. 514, No. 7520, 2014, pp. 68–71.

[20] P. Lucey, B. Hawke, C. Pieters, J. Head, and T. McCord, "A compositional study of the Aristarchus region of the Moon using near-infrared reflectance spectroscopy," *Lunar and Planetary Science Conference Proceedings*, Vol. 16, 1986, p. 344.

[21] J. Head and L. Wilson, "The formation of eroded depressions around the sources of lunar sinuous rilles: Observations," *Lunar and Planetary Science Conference*, Vol. 11, 1980, pp. 426–428.

[22] W. B. Garry and J. E. Bleacher, "Emplacement scenarios for Vallis Schröteri, Aristarchus Plateau, the Moon," *Geological Society of America Special Papers*, Vol. 477, 2011, pp. 77–93.

[23] L. J. Porcello, R. L. Jordan, J. S. Zelenka, G. F. Adams, R. J. Phillips, W. E. Brown Jr, S. H. Ward, and P. L. Jackson, "The Apollo lunar sounder radar system," *Proceedings of the IEEE*, Vol. 62, No. 6, 1974, pp. 769–783.

[24] J. Mouginot, A. Pommerol, P. Beck, W. Kofman, and S. M. Clifford, "Dielectric map of the Martian northern hemisphere and the nature of plain filling materials," *Geophysical research letters*, Vol. 39, No. 2, 2012.

[25] N. E. Putzig, R. J. Phillips, B. A. Campbell, M. T. Mellon, J. W. Holt, and T. C. Brothers, "SHARAD soundings and surface roughness at past, present, and proposed landing sites on Mars: Reflections at Phoenix may be attributable to deep ground ice," *Journal of Geophysical Research: Planets*, Vol. 119, aug 2014, pp. 1936–1949, 10.1002/2014je004646.

[26] A. Pommerol, W. Kofman, J. Audouard, C. Grima, P. Beck, J. Mouginot, A. Herique, A. Kumamoto, T. Kobayashi, and T. Ono, "Detectability of subsurface interfaces in lunar maria by the LRS/SELENE sounding radar: Influence of mineralogical composition," *Geophysical Research Letters*, Vol. 37, No. 3, 2010.

[27] Y. Su, G.-Y. Fang, J.-Q. Feng, S.-G. Xing, Y.-C. Ji, B. Zhou, Y.-Z. Gao, H. Li, S. Dai, Y. Xiao, *et al.*, "Data processing and initial results of Chang'e-3 lunar penetrating radar," *Research in Astronomy and Astrophysics*, Vol. 14, No. 12, 2014, p. 1623.

[28] G.-Y. Fang, B. Zhou, Y.-C. Ji, Q.-Y. Zhang, S.-X. Shen, Y.-X. Li, H.-F. Guan, C.-J. Tang, Y.-Z. Gao, W. Lu, *et al.*, "Lunar Penetrating Radar onboard the Chang'e-3 mission," *Research in Astronomy and Astrophysics*, Vol. 14, No. 12, 2014, p. 1607.

[29] L. Bruzzone, G. Alberti, C. Catallo, A. Ferro, W. Kofman, and R. Orosei, "Subsurface radar sounding of the Jovian moon Ganymede," *Proceedings of the IEEE*, Vol. 99, No. 5, 2011, pp. 837–857.

[30] R. Seu, D. Biccari, R. Orosei, L. Lorenzoni, R. Phillips, L. Marinangeli, G. Picardi, A. Masdea, and E. Zampolini, "SHARAD: The MRO 2005 shallow radar," *Planetary and Space Science*, Vol. 52, No. 1, 2004, pp. 157–166.

[31] B. Cooper, "Apollo 17 Lunar Sounder Data Provide Insight into Aitken Crater's Subsurface Structure," *Lunar and Planetary Science Conference*, Vol. 39, 2008, p. 2369.

[32] T. Ono and H. Oya, "Lunar Radar Sounder (LRS) experiment on-board the SELENE spacecraft," *Earth, planets and space*, Vol. 52, No. 9, 2000, pp. 629–637.

[33] M. Zuber, D. Smith, S. Asmar, A. Konopliv, F. Lemoine, H. Melosh, G. Neumann, R. Phillips, S. Solomon, M. Watkins, *et al.*, "Gravity Recovery and Interior Laboratory (GRAIL): extended mission and endgame status," *Lunar and Planetary Science Conference*, Vol. 44, 2013, p. 1777.

[34] F. G. Lemoine, S. Goossens, T. J. Sabaka, J. B. Nicholas, E. Mazarico, D. D. Rowlands, B. D. Loomis, D. S. Chinn, G. A. Neumann, D. E. Smith, *et al.*, "GRGM900C: A degree 900 lunar gravity model from GRAIL primary and extended mission data," *Geophysical Research Letters*, Vol. 41, No. 10, 2014, pp. 3382–3389.

[35] A. S. Konopliv, R. S. Park, D.-N. Yuan, S. W. Asmar, M. M. Watkins, J. G. Williams, E. Fahnestock, G. Kruizinga, M. Paik, D. Strekalov, *et al.*, "High-resolution lunar gravity fields from the GRAIL Primary and Extended Missions," *Geophysical Research Letters*, Vol. 41, No. 5, 2014, pp. 1452–1458.